Fundamental and Applied Laser Physics: Proceedings of the
Esfahan Symposium August 29- September 5, 1971
Edited by M. S. Feld, A. Javan and N. Kurnit

TRANSVERSE OPTICAL PUMPING AND LEVEL CROSSINGS IN FREE AND "DRESSED" ATOMS

C. Cohen-Tannoudji
Laboratoire de Physique de l'Ecole Normale Supérieure,
Université de Paris, Paris, France

I. INTRODUCTION

One of the important characteristics of optical pumping is to provide the possibility of preparing an atomic system in a coherent superposition of Zeeman sublevels [1]. For a $J = 1/2$ angular momentum state, it is equivalent to say that the magnetization $\vec{M}_0$ introduced by the pumping light is not necessarily parallel to the static magnetic field $\vec{B}_0$ (as is usually the case when $\vec{M}_0$ is determined only by the Boltzmann factor in $\vec{B}_0$).

Using such a "transverse" pumping, one can observe level crossing signals in atomic ground states. The width of the observed level crossing resonances may be extremely small as I will show in the first part of this paper. Some possible applications to the detection of very weak magnetic fields will be described.

I will then study the modifications which appear on optical pumping signals when the atoms are no longer free but interacting with nonresonant radio-frequency (rf) photons. These interactions may be visualized in terms of virtual absorptions and reemissions of rf quanta, leading to some sort of "dressing" of the atom by the surrounding quanta. The Zeeman diagram of the "dressed atom" is more complex than the one of the corresponding free atom. The level crossings which were present on the free atom are considerably modified. New level crossings appear. All these effects can be

studied by optical pumping techniques as I will show in the second part of this paper.

It may appear surprising to quantize a rf field which is essentially classical and, effectively, all the effects I will describe could be understood in a classical way. I think however that the quantization of the rf field introduces a great simplification in the theory as it leads to a time-independent Hamiltonian for the whole isolated system atom + rf field, much easier to deal with than the time-dependent Hamiltonian of the classical theory. In particular, all the higher-order effects such as multiple quanta transitions, Bloch-Siegert type shifts, Autler-Townes splitting, etc., appear clearly on the Zeeman diagram of the dressed atom. Consequently, this approach could perhaps be generalized to the study of some of the nonlinear phenomena observable with intense laser light.

II. LEVEL CROSSING RESONANCES IN ATOMIC GROUND STATES AND DETECTION OF VERY WEAK MAGNETIC FIELDS

It is well known that the resonance radiation scattered by an atomic vapor exhibits resonant variations when the static field is scanned around values corresponding to a crossing between two Zeeman sublevels of the excited state (Hanle effect - Franken effect) [2]. The width of these resonances is the natural width of the excited state, not the Doppler width. They give useful informations about this state, such as lifetimes, g factors, hyperfine structure [3], etc.

Similar resonances, with a considerably smaller width, can be observed in atomic ground states [4]. To simplify, we will consider a $J = 1/2$ angular momentum state (the calculations could be easily generalized to higher J's). The pumping beam is circularly polarized and propagates along the Ox direction, perpendicularly to the static field $\vec{B}_o$, which is parallel to Oz (Fig. 1).

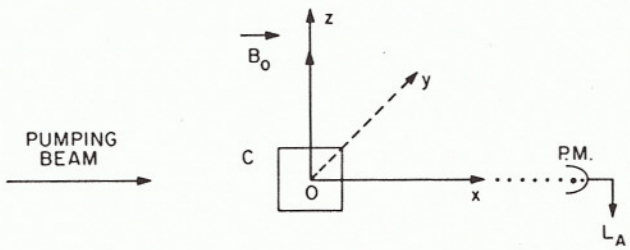

Figure 1. Schematic diagram of the experimental arrangement for the observation of level crossing resonances in atomic ground states. $\vec{B}_o$: static field; P.M.: photomultiplier measuring the absorbed light L_A; C: resonance cell.

As a result of the optical pumping cycle, angular momentum is transferred from the incident quanta to the atoms contained in the resonance cell C. Let $\vec{M}$ be the total magnetization of the vapor. It is easy to derive the following equation of evolution for $\vec{M}$:

$$\frac{d}{dt}\vec{M} = \frac{\vec{M}_o - \vec{M}}{T_P} - \frac{\vec{M}}{T_R} + \gamma \vec{M} \times \vec{B}_o \tag{1}$$

The first term represents the effect of optical pumping: if this process was the only one, after a certain amount of time T_P (pumping time), all the spins would be pointing in the Ox direction, producing a saturation magnetization $\vec{M}_o$ parallel to Ox; the second term describes the thermal relaxation process (T_R: relaxation time) due to the collisions against the walls of the cell; the third term, the Larmor precession around $\vec{B}_o$ (γ is the gyromagnetic ratio of the ground state).

Equation (1) looks like the well-known Bloch's equation. But here, $\vec{M}_o$ is not along $\vec{B}_o$ and its direction is imposed by the characteristics of the pumping beam.

Defining

$$M_\pm = M_x \pm iM_y \tag{2}$$

$$\frac{1}{\tau} = \frac{1}{T_P} + \frac{1}{T_R} \tag{3}$$

$$M'_o = M_o \frac{\tau}{T_P}$$

one gets from (1)

$$\frac{d}{dt} M_z = 0 \tag{4a}$$

$$\frac{d}{dt} M_\pm = \frac{M'_o}{\tau} - \frac{M_\pm}{\tau} \mp i\gamma B_o M_\pm \tag{4b}$$

Note that the source term, M'_o/τ, proportional to M_o, appears only in Eq. (4b) relative to the transverse components of the magnetization (transverse pumping).

The steady-state solution of (4) is readily obtained and can be written as

$$M_z = 0 \tag{5a}$$

$$M_\pm = \frac{M'_o}{1 \pm i\gamma \tau B_o} \tag{5b}$$

which gives

$$M_z = 0 \tag{6a}$$

$$\frac{M_x}{M'_o} = \frac{1}{1 + (\gamma \tau B_o)^2} \tag{6b}$$

$$\frac{M_y}{M'_o} = \frac{-\gamma \tau B_o}{1 + (\gamma \tau B_o)^2} \tag{6c}$$

It follows that M_x and M_y undergo resonant variations when B_o is scanned around 0 (Fig. 2).

These variations result from the competition between optical pumping which tends to orient the spins along the Ox axis and the Larmor precession around $\vec{B}_o$. The critical value of the field, ΔB_o, for which the two processes have the same importance is given by

$$\Delta B_o = 1/\gamma \tau \tag{7}$$

ΔB_o is the half-width of the resonances of Fig. 2, which can be detected by monitoring the absorbed or reemitted light, the characteristics of which (intensity, degree of polarization) depend on M_x, M_y, M_z. For example, the photomultiplier P.M. of Fig. 1 detects the absorbed light L_A which is proportional to M_x.

It is possible to get modulated signals by adding a high-frequency rf field $\vec{B}_1 \cos\omega t$ parallel to $\vec{B}_o$ (high frequency means nonadiabatic modulation: $\omega \gg 1/\tau$). The rate equations in the presence of $\vec{B}_1 \cos\omega t$ can be exactly solved [5]. One finds that the zero-field level crossing resonances appear

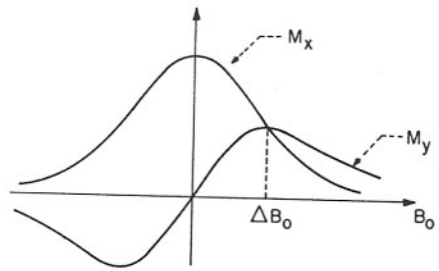

Figure 2. Variations of the steady-state values of M_x and M_y with B_o. ΔB_o: half-width of the resonances.

also on modulations at the various harmonics $p\omega$ of ω ($p = 1, 2, 3 \ldots$). For example, the ω component of M_x is given around $B_o = 0$ by

$$M_x(\omega) = M'_o J_0\left(\frac{\gamma B_1}{\omega}\right) J_1\left(\frac{\gamma B_1}{\omega}\right) \frac{\gamma \tau B_o}{1+(\gamma \tau B_o)^2} \sin\omega t \tag{8}$$

where J_0 and J_1 are the Bessel functions of order 0 and 1. It varies with B_o as a dispersion curve. The possibility of using selective amplification and lock-in detection techniques with such a signal, increases considerably the signal-to-noise ratio.

Let us calculate the order of magnitude of ΔB_o for ^{87}Rb which has been experimentally studied [5]. In paraffin-coated cells [6] without buffer gas, T_R (and consequently τ) is of the order of 1 sec; γ is equal to 4.4×10^6 rad sec^{-1} G^{-1}, so that $\Delta B_o \simeq 10^{-6}$G. Clearly, with such a small width, one has to operate inside a magnetic shield in order to eliminate the erratic fields present in the laboratory (of the order of 10^{-3}G). Five concentric layers of mu-metal (1 m long, 50 cm in diameter, 2 mm thick) have been used for that purpose, providing sufficient protection.

Figure 3 shows an example of the level crossing resonance observed on the modulation at ω of the absorbed light, i.e., on the signal corresponding to theoretical expression (8) ($\omega/2\pi = 400$ Hz). The time constant of the detection is 3 sec. We get a 2-μG width and a signal-to-noise ratio of the order of 3000. It is therefore possible to detect very weak magnetic fields (less than 10^{-9}G) as it appears in Fig. 4 which shows the response of the signal to square pulses of 2×10^{-9} G amplitude around $B_o = 0$.

Such a high sensitivity is sufficient to measure the static magnetization of very dilute substances. Suppose one places near the ^{87}Rb cell another cell (6 cm in diameter) containing ^{3}He gas at a pressure of 3 Torr (Fig. 5).

The ^{3}He nuclei are optically pumped [7] by a ^{3}He beam B_2, to a 5% polarization. One calculates easily that the oriented ^{3}He nuclei produce at the center of the ^{87}Rb cell (6 cm away) a macroscopic field of the order of 6×10^{-8} G. This field is sufficiently large to be detected on the ^{87}Rb level crossing signal obtained on the B_1 beam.

The experiment has been done [8] and Fig. 6 shows the modulation of the ^{87}Rb signal due to the free precession of the ^{3}He nuclear spins around a small magnetic field applied only on the ^{3}He cell, perpendicular to the directions of B_1 and B_2 (the Larmor period is of the order of 2 min). One sees that one can follow the free decay of the ^{3}He magnetization during hours and hours until it corresponds to only 5×10^{13} oriented nuclei per cm^3. This magnetostatic detection presents many advantages compared to the other optical or radioelectric methods. It could be generalized to other cases (for example to optically pumped centers in solids or to weakly magnetized geological samples). Other spatial or biological applications

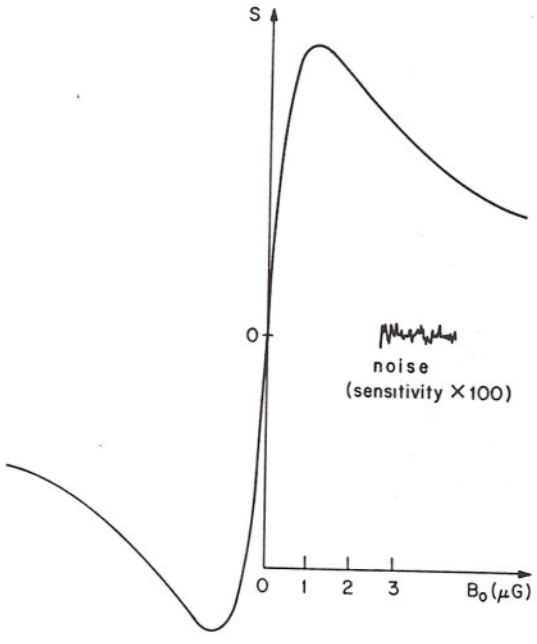

Figure 3. Zero-field level crossing resonance in the ground state of ^{87}Rb observed on the modulation at $\omega/2\pi$ of the absorbed light L_A ($\omega/2\pi = 400$ Hz). The time constant of the detection is 3 sec. For measuring the noise, the sensitivity is multiplied by a factor 100.

could be considered as it is now possible, by recent improvements [9], to record simultaneously the three components of the small magnetic field to be measured.

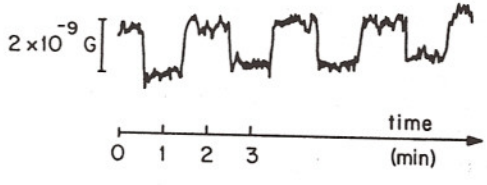

Figure 4. Test of the sensitivity of the magnetometer: variations of the signal when square pulses of 2×10^{-9} G are applied to the resonance cell.

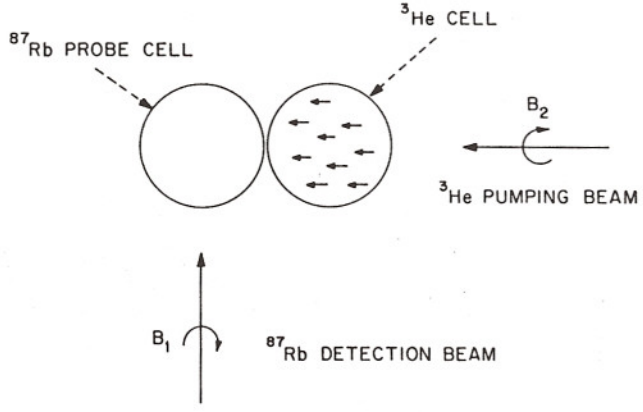

Figure 5. Detection by the ^{87}Rb level crossing resonance of the magnetic field produced at a macroscopic distance (6 cm) by optically pumped ^{3}He nuclei. Schematic diagram of the experimental arrangement.

III. OPTICAL PUMPING OF "DRESSED" ATOMS

To interpret the various resonances which appear in optical pumping experiments performed on atoms interacting with strong resonant or nonresonant rf fields, we will try to develop the following general idea [10, 11]: the light of the pumping beam is scattered, not by the free atom, but by the whole system--atom + rf field in interaction--which we will call the atom "dressed" by rf quanta. Plotted as a function of the static field B_0, the Zeeman diagram of this dressed atom exhibits a lot of crossing and anticrossing points; as for a free atom, the light scattered by such a system undergoes resonant variations when B_0 is scanned around these points. It is therefore possible to understand the various resonances appearing in optical pumping experiments in a very synthetic way. Furthermore, the higher-order effects of the coupling between the atom and the rf field may be handled in a simple way, by time-independent perturbation theory. In some cases (as for example for the modification of the g factor of the dressed atom), the effect of the coupling may be calculated to all orders.

In the absence of coupling, the energy levels of the whole system are labelled by two quantum numbers, one for the atom (we will take a two-level system, $J = 1/2$), and the other for the field. We will call $|\pm\rangle$ the Zeeman sublevels of the $J = 1/2$ atomic state; their energy in the presence of a

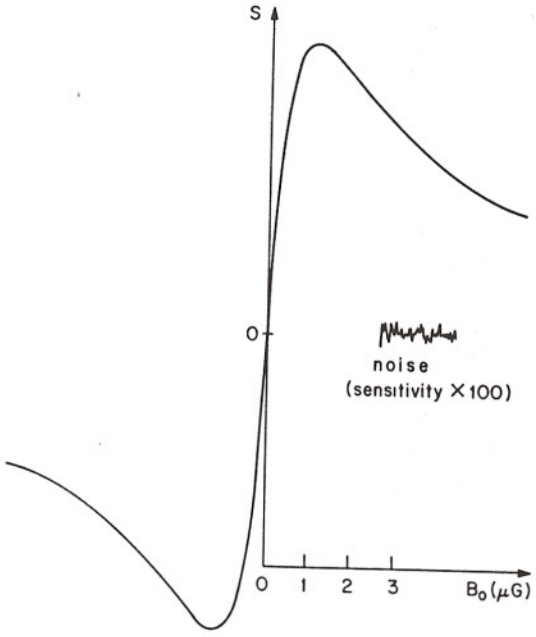

Figure 3. Zero-field level crossing resonance in the ground state of ^{87}Rb observed on the modulation at $\omega/2\pi$ of the absorbed light L_A ($\omega/2\pi$ = 400 Hz). The time constant of the detection is 3 sec. For measuring the noise, the sensitivity is multiplied by a factor 100.

could be considered as it is now possible, by recent improvements [9], to record simultaneously the three components of the small magnetic field to be measured.

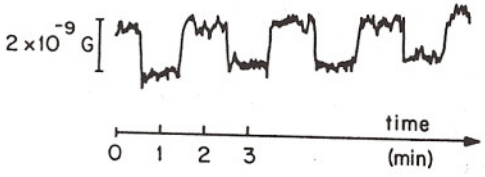

Figure 4. Test of the sensitivity of the magnetometer: variations of the signal when square pulses of 2×10^{-9} G are applied to the resonance cell.

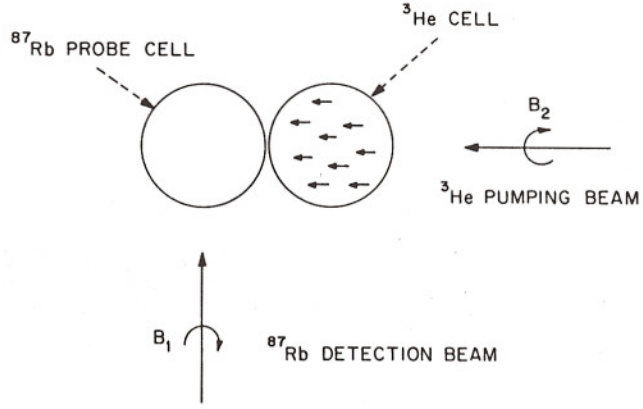

Figure 5. Detection by the ^{87}Rb level crossing resonance of the magnetic field produced at a macroscopic distance (6 cm) by optically pumped ^{3}He nuclei. Schematic diagram of the experimental arrangement.

III. OPTICAL PUMPING OF "DRESSED" ATOMS

To interpret the various resonances which appear in optical pumping experiments performed on atoms interacting with strong resonant or nonresonant rf fields, we will try to develop the following general idea [10, 11]: the light of the pumping beam is scattered, not by the free atom, but by the whole system--atom + rf field in interaction--which we will call the atom "dressed" by rf quanta. Plotted as a function of the static field B_0, the Zeeman diagram of this dressed atom exhibits a lot of crossing and anticrossing points; as for a free atom, the light scattered by such a system undergoes resonant variations when B_0 is scanned around these points. It is therefore possible to understand the various resonances appearing in optical pumping experiments in a very synthetic way. Furthermore, the higher-order effects of the coupling between the atom and the rf field may be handled in a simple way, by time-independent perturbation theory. In some cases (as for example for the modification of the g factor of the dressed atom), the effect of the coupling may be calculated to all orders.

In the absence of coupling, the energy levels of the whole system are labelled by two quantum numbers, one for the atom (we will take a two-level system, J = 1/2), and the other for the field. We will call $|\pm\rangle$ the Zeeman sublevels of the J = 1/2 atomic state; their energy in the presence of a

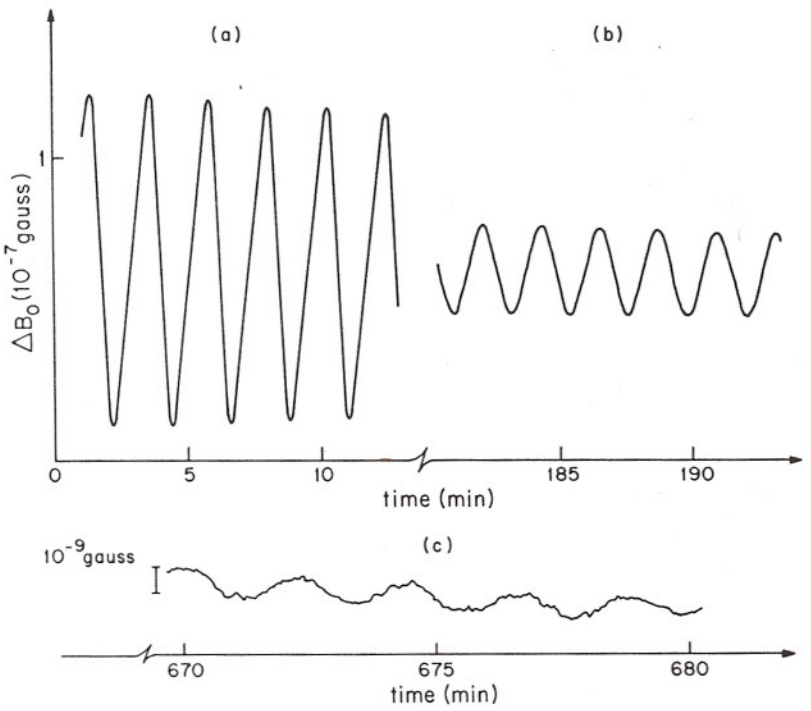

Figure 6. Magnetostatic detection of the Larmor precession of ^{3}He nuclei: (a) just after optical pumping has been stopped; (b) 3 h later; (c) 11 h later (the polarization is now $P \simeq 5 \times 10^{-4}$ and corresponds to 5.3×10^{13} oriented nuclei per cm^3).

static field B_0 parallel to Oz is $\pm \omega_0/2$ ($\omega_0 = -\gamma B_0$; we take $\hbar = 1$). Let $|n\rangle$ be the states of the rf field corresponding to the presence of n quanta and consequently to an energy $n\omega$ (ω is the pulsation of the rf field). The states of the combined system atom + field (without coupling) are the $|\pm, n\rangle$ states with an energy $\pm\omega_0/2 + n\omega$. They are plotted on Fig. 7 versus ω_0. One sees that a lot of crossing points appear for $\omega_0 = 0, \omega, 2\omega, 3\omega, \ldots$. The effect of the coupling V between the atom and the rf field is important at these points. We will first study this coupling in a simple and exactly soluble case, the one of a rotating rf field, perpendicular to $\vec{B}_0$ (this situation leads also to exact solutions in the classical theory).

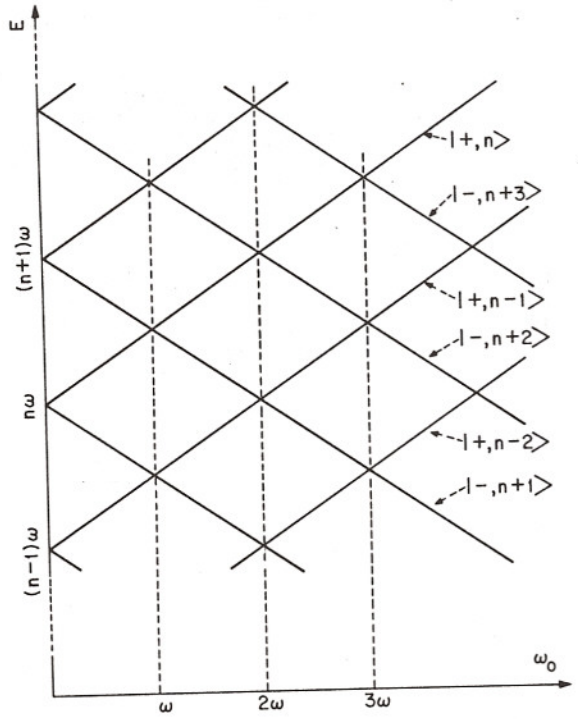

Figure 7. Energy levels of the combined system "atom + rf field" in the absence of coupling.

A. Rotating rf Field Perpendicular to $\vec{B}_0$

The unperturbed states are coupled two by two by V. For example, the $|-, n+1\rangle$ state is coupled only to $|+, n\rangle$ and the other way

$$|-, n+1\rangle \longleftrightarrow |+, n\rangle$$

The physical meaning of such a selection rule is very clear. Each circularly polarized rf quantum carries an angular momentum +1 with respect to Oz (σ^+ photons; we suppose a right circular polarization) and the two states coupled by V must have the same total angular momentum: $-1/2 + (n+1) = +1/2 + n$.

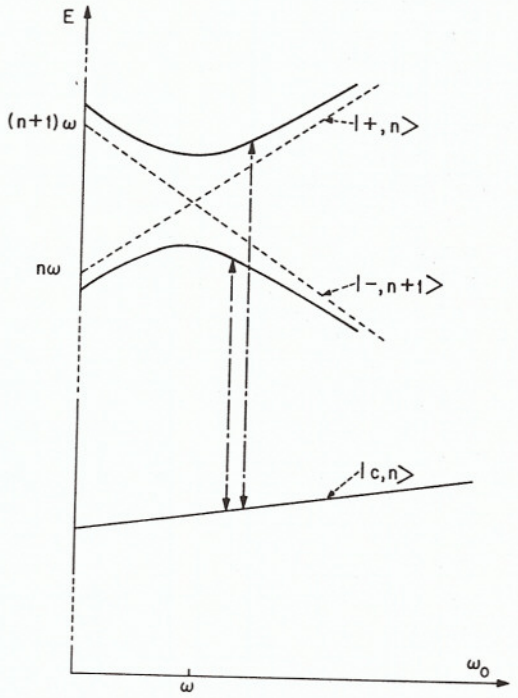

Figure 8. "Anticrossing" resulting from the coupling between the two states $|+,n\rangle$ and $|-,n+1\rangle$. The dotted arrows represent transitions between the two anticrossing levels and a third level (Autler-Townes splitting).

Because of this coupling, the two unperturbed states which cross for $\omega_0 = \omega$ (dotted lines of Fig. 8) repel each other and form what is called an "anticrossing" (full lines of Fig. 8). The minimum distance between the two branches of the hyperbola is obtained for $\omega_0 = \omega$ and is proportional to the matrix element of V between the two unperturbed states. It is possible to show that this matrix element v is proportional to $\sqrt{n+1}$ and may be related to the amplitude B_1 of the classical rf field (more precisely, v is proportional to $\omega_1 = -\gamma B_1$). As n is very large, this matrix element does not change appreciably when n is varied inside the width Δn of the distribution p(n) corresponding to the rf field (for a coherent state [12], $\Delta n \ll n$). Therefore, the anticrossings corresponding to the couples of unperturbed states, $(|-,n+2\rangle, |+,n+1\rangle)$, $(|-,n\rangle, |+,n-1\rangle)$,..., have the same characteristics

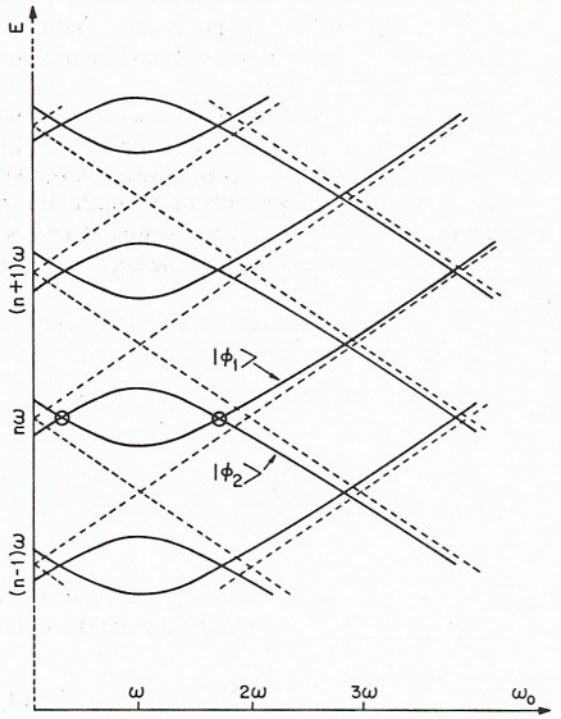

Figure 9. Energy levels of the combined system "atom + rf field" in the presence of coupling. The rf field is circularly polarized and perpendicular to the static field $\vec{B}_0$.

as the one of Fig. 8 (they are deduced from it by a simple vertical translation) and we obtain finally the Zeeman diagram of Fig. 9.

What kind of information can be extracted from this diagram? First, the anticrossings of Fig. 9 reveal the existence of the magnetic resonance occuring for $\omega_0 = \omega$. If one starts from the state $|-,n+1\rangle$, the system is transferred by the coupling V to the other state $|+,n\rangle$ (transition $|-\rangle \rightarrow |+\rangle$ by absorption of one rf quantum). More precisely, the system oscillates between these two states with an efficiency maximum at the center of the anticrossing (where the mixing between the two unperturbed states is maximum) and at a frequency corresponding to the distance between the two branches of the hyperbola (this is nothing but the well-known Rabi precession). If one looks at the frequencies of the transitions joining the

two anticrossing levels of Fig. 8 to a different atomic level $|c,n\rangle$ (not resonantly coupled to the rf field), one finds a doublet (Autler-Townes effect) [13]; the distance between the two components of the doublet and their relative intensities are very simply related to the energies and wave functions of the two anticrossing levels.

A lot of crossing points appear also on the energy diagram of Fig. 9. Let us focus on the two crossings indicated by circles on this figure. The zero-field level crossing of the free atom is shifted by the coupling V; a new level crossing appears near $\omega_0 = 2\omega$ and can be optically detected in transverse optical pumping experiments. The argument is the following: let $|\varphi_1\rangle$ and $|\varphi_2\rangle$ be the two perturbed crossing levels; we have

$$|\varphi_1\rangle = -\sin(\theta/2)|+,n-1\rangle + \cos(\theta/2)|-,n\rangle$$
$$|\varphi_2\rangle = \sin(\theta/2)|-,n+1\rangle + \cos(\theta/2)|+,n\rangle \tag{10}$$

where

$$\tan\theta = \frac{-\gamma B_1}{\omega_0 - \omega} \tag{11}$$

$|\varphi_1\rangle$ and $|\varphi_2\rangle$ contain admixtures of the $|+,n\rangle$ and $|-,n\rangle$ states which correspond to the same value of n so that they can be connected by J_x

$$\langle \varphi_2 | J_x | \varphi_1 \rangle = \cos^2(\theta/2)\, \langle n|n\rangle\, \langle + | J_x | - \rangle$$
$$= (1/2)\cos^2(\theta/2) \neq 0 \tag{12}$$

It is therefore possible to introduce by optical pumping a transverse static magnetization at this crossing point and to get a level crossing signal of the same type as the one described in the first part of this paper (for the other crossings of Fig. 9: $\omega_0 = 3\omega, 4\omega, 5\omega, \ldots$, J_x has no matrix elements between the two crossing perturbed levels, and the level crossings are not detectable).

When the intensity of the rf field (i.e., n) is increased, the distance between the two branches of the hyperbola of Fig. 8 increases and the two crossings of Fig. 9 (indicated by circles) shift towards $\omega_0 = \omega$. These effects appear clearly on Fig. 10 which represents the two corresponding level crossing resonances observed on ^{199}Hg (J = 1/2) [14]. Each curve of figure 10 corresponds to a different value of the amplitude of the rf field (measured by the dimensionless parameter $\omega_1/\omega = -\gamma B_1/\omega$).

Finally, it can be seen in Fig. 9 that, for $\omega_0 = 0$, the Zeeman degeneracy of the free atom is removed by the coupling with the nonresonant circularly polarized rf field. One can show [15] that, for $\omega_1/\omega \ll 1$, the effect of this coupling is equivalent to that of a fictitious static field $\vec{B}_f$ perpendicular to the plane of the rf field and proportional to $\omega_1^2/\gamma\omega$

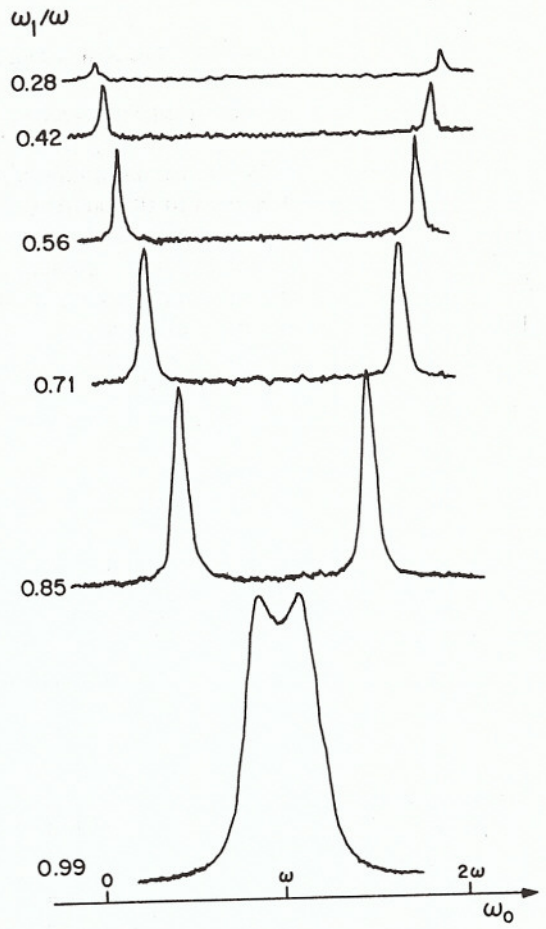

Figure 10. Level crossing resonances observed on ^{199}Hg and corresponding to the two-level crossings indicated by circles on Fig. 9. Each curve corresponds to a different value of the dimensionless parameter ω_1/ω.

$$B_f = \omega_1^2/\gamma\omega \tag{13}$$

In the case of an alkali atom such as ^{87}Rb which has two hyperfine levels in the ground state, F = 2 and F = 1, with two opposite g factors ($\gamma_2 = -\gamma_1$), it follows from (13) that the two fictitious fields B_{f_2} and B_{f_1} corresponding to F = 2 and F = 1 are opposite. Therefore, the position of the Zeeman sublevels in the presence of rf irradiation (and in zero static field) is the one shown on Fig. 11(b); it may be compared to the position of the Zeeman sublevels in a true static field producing the same Zeeman separation [Fig. 11(a)]. It follows immediately that the hyperfine spectrum is completely different in a true static field and in the fictitious fields B_{f_1} and B_{f_2} associated with the rf field: we obtain experimentally [15] three $\Delta m_F = 0$ and four $\Delta m_F = \pm 1$ different lines in the first case [Figs. 12(a) and 13(a)]; one $\Delta m_F = 0$ and two $\Delta m_F = \pm 1$ different lines in the second case, as for hydrogen [Figs. 12(b) and 13(b)].

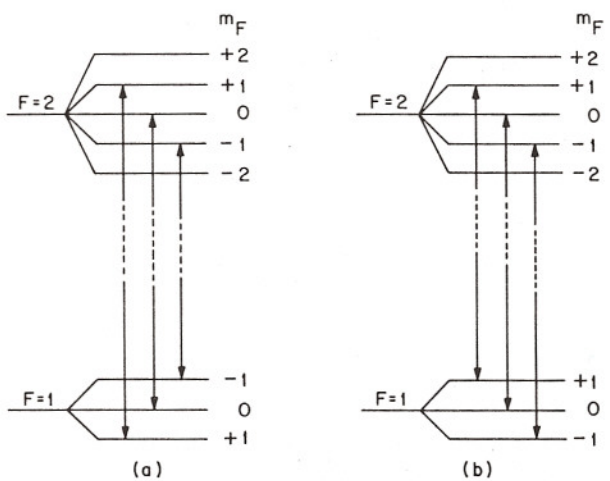

Figure 11. Zeeman sublevels in the ground state of ^{87}Rb atoms, (a) in the presence of a true static field $\vec{B}_o$, (b) in the presence of a circularly polarized rf field with $\vec{B}_o = 0$; the two fictitious static fields $\vec{B}_{f_1}$ and $\vec{B}_{f_2}$ describing the effect of this rf field inside the F = 1 and F = 2 hyperfine levels are opposite. The arrows represent the three $\Delta m_F = 0$ hyperfine lines which have different frequencies in case (a) and which coincide in case (b).

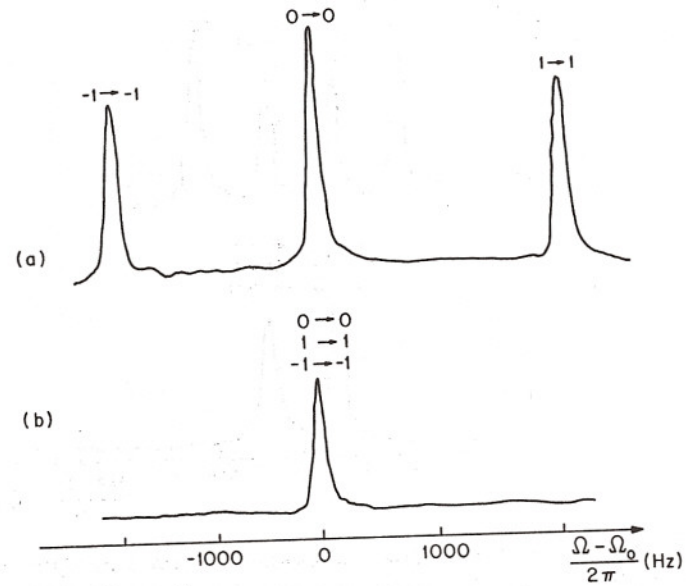

Figure 12. $\Delta m_F = 0$ hyperfine transitions observed on ^{87}Rb atoms, (a) in a true static field $\vec{B}_o$ [see Fig. 11(a)], (b) in the presence of a circularly polarized rf field with $\vec{B}_o = 0$ [see Fig. 11(b)].

B. Linear rf Field Perpendicular to $\vec{B}_o$

We suppose now that the rf field has a linear polarization, perpendicular to $\vec{B}_o$ (Fig. 14). Such a linear field can be decomposed into two σ^+ and σ^- rotating components. It is equivalent to say that each of the rf quanta has no definite angular momentum with respect to Oz : this angular momentum may be either +1 (σ^+ component) or -1 (σ^- component).

Consequently, the unperturbed $|-,n+1\rangle$ state is now coupled, not only to $|+,n\rangle$ (absorption of a σ^+ photon), but also to $|-,n+2\rangle$ (stimulated emission of a σ^- photon); similarly, the $|+,n\rangle$ state is coupled not only to $|-,n+1\rangle$, but also to $|-,n-1\rangle$

$$\begin{array}{ccc} |+,n\rangle & \xleftrightarrow{\sigma^+} & |-,n+1\rangle \\ \sigma^- \uparrow \downarrow & & \uparrow \downarrow \sigma^- \\ |-,n-1\rangle & & |+,n+2\rangle \end{array} \tag{14}$$

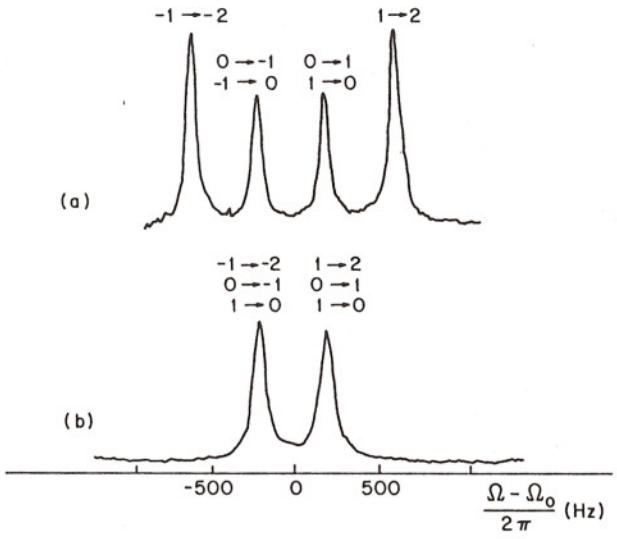

Figure 13. $\Delta m_F = \pm 1$ hyperfine transitions observed on ^{87}Rb atoms, (a) in a true static field $\vec{B}_0$, (b) in the presence of a circularly polarized rf field with $\vec{B}_0 = 0$.

These additional couplings which were not present in the previous case (pure σ^+ rf field) are nonresonant for $\omega_0 = \omega$ (the two $|-,n-1\rangle$ and $|+,n+2\rangle$ states do not have the same energy as the two crossing unperturbed levels). They displace however these two crossing levels (from the position indicated by dotted lines in Fig. 15 to the one indicated by interrupted lines) so that the center of the anticrossing $\omega_0 = \omega$ (full lines of Fig. 15) is now shifted by a quantity δ towards $\omega_0 = 0$. This shift δ is nothing but the well-known Bloch-Siegert shift which is immediately evaluated in this formalism by elementary second-order perturbation theory (the derivation of this shift is much more

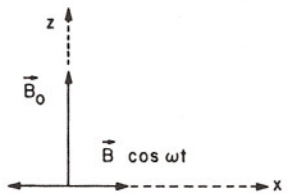

Figure 14. Orientation of the static and rf fields.

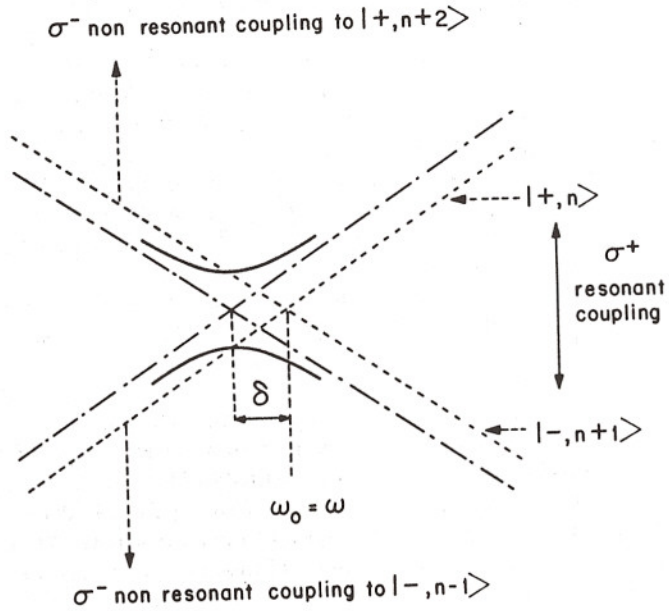

Figure 15. Origin of the Bloch-Siegert shift observed when the rf field has a linear polarization : nonresonant couplings (dotted arrows) are induced by the σ^- component of the rf field and displace the two anticrossing levels.

elaborate in classical theory) [16]. We must also notice that the two unperturbed levels which cross for $\omega_0 = -\omega$ (for example $|-,n+1\rangle$ and $|+,n+2\rangle$) are now coupled by the σ^- component of the rf field. This gives rise to a new anticrossing near $\omega_0 = -\omega$ (symmetrical to the first one with respect to $\omega_0 = 0$).

Moreover, one can easily show that each "odd" crossing $\omega_0 = (2p+1)\omega$ (with $p = +1, +2, \ldots$) appearing in Fig. 7 becomes now anticrossing. Let us consider for example the case of the two levels $|-,n+2\rangle$ and $|+,n-1\rangle$ which cross for $\omega_0 = 3\omega$

$$\begin{array}{ccccccc} |+,n-1\rangle & \overset{\sigma^+}{\longleftrightarrow} & |-,n\rangle & \overset{\sigma^-}{\longleftrightarrow} & |+,n+1\rangle & \overset{\sigma^+}{\longleftrightarrow} & |-,n+2\rangle \\ \sigma^- \updownarrow & & & & & & \sigma^- \updownarrow \\ |-,n-2\rangle & & & & & & |+,n+3\rangle \end{array} \qquad (15)$$

As shown in (15), they are coupled by V, not directly, but through two intermediate states. It follows that the crossing $\omega_0 = 3\omega$ becomes a "third-order anticrossing" (which is also shifted towards $\omega_0 = 0$, as the $\omega_0 = \omega$ anticrossing, as a consequence of nonresonant couplings).

The even crossings $\omega_0 = 2p\omega$ ($p = 0, 1, 2, \ldots$) of Fig. 7 remain however true crossings (which are also shifted for the same reason as before towards $\omega_0 = 0$). The argument is the following: for $\omega_0 = 2p\omega$, the two crossing levels (for example, $|+, n\rangle$ and $|-, n+2p\rangle$) differ by 2p quanta. The absorption of an even number of quanta (σ^+ or σ^-) cannot provide the angular moment +1 necessary for the atomic transition $|-\rangle \rightarrow |+\rangle$. This excludes any direct or indirect coupling between the two crossing levels.

Finally, through these simple arguments, we get the shape of the Zeeman diagram represented in full lines in Fig. 16 and which is symmetrical with respect to $\omega_0 = 0$ (the crossing $\omega_0 = 0$ is not shifted as in the previous case). All the various resonances observable in optical pumping experiments appear in a synthetic way in this diagram.

To the various anticrossings of Fig. 16 are associated the magnetic resonances involving one or several rf quanta [17]. For example, near $\omega_0 = 3\omega$, we have a resonant oscillation of the system between the two states $|-, n+2\rangle$ and $|+, n-1\rangle$ which correspond to resonant transitions between $|-\rangle$ and $|+\rangle$ with absorption of three rf quanta. The shift and the rf broadening of the resonances are simply related to the position of the center

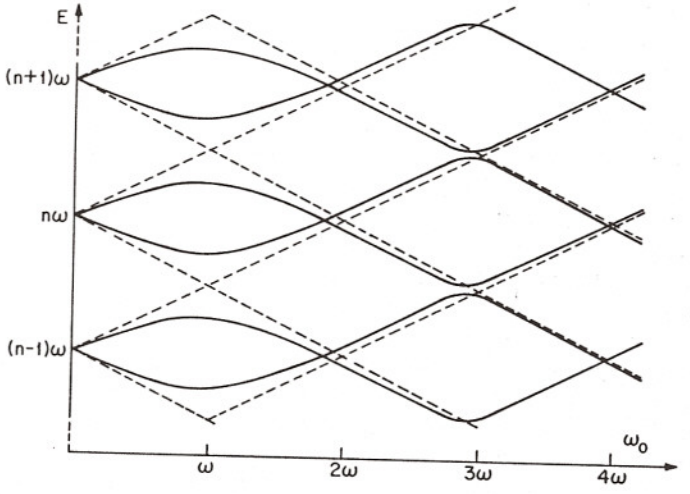

Figure 16. Energy levels of the combined system "atom + rf field" in the presence of coupling. The rf field is linearly polarized and perpendicular to the static field $\vec{B}_0$.

of the anticrossing and to the minimum distance between the two branches of the hyperbola. It is also clear that an Autler-Townes splitting must appear near these higher-order anticrossings.

All the even crossings of Fig. 16 can be detected in transverse optical pumping experiments : in the perturbation expansion of the two crossing perturbed levels, one can find unperturbed states with the same value of n so that J_x can connect the two crossing levels. Figure 17 shows for example the $\omega_0 = 4\omega$ level crossing resonance observed on ^{199}Hg atoms [18]. (This resonance does not appear with a pure σ^+ rf field). Each curve corresponds to an increasing value of the rf amplitude. The Bloch-Siegert type shift appears very clearly. Such resonances are sometimes called "parametric" resonances or "coherence" resonances as they do not correspond to real absorptions of one or several rf quanta by the atomic system.

So far, we have explicitly treated the effect of the coupling V as a perturbation. It is possible to follow qualitatively what happens in the neighborhood of $\omega_0 = 0$ when the amplitude of the rf field is increased. The first crossings $\omega_0 = +2\omega$ and $\omega_0 = -2\omega$ shift more and more towards $\omega_0 = 0$. The separation between the two branches of the anticrossing $\omega_0 = \omega$ increases more and more. It follows that the slope of the two levels which cross for $\omega_0 = 0$, i.e., the g factor of the dressed atom, gets smaller and smaller.

More precisely, it is possible to find exactly the eigenstates of the Hamiltonian $\mathcal{H}_{rf} + V$ which represents the energy of the system in zero static field [19] ($\mathcal{H}_{rf}$ is the energy of the free rf field) and to treat the Zeeman term $\mathcal{H}_{at} = \omega_0 J_z$ as a perturbation. This treatment, which takes into account the effect of the coupling to all orders, gives the slope of the levels as a function of the dimensionless parameter ω_1/ω. One finds [20]

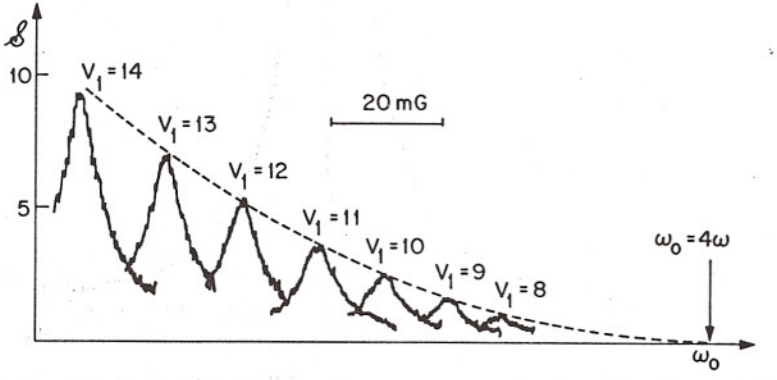

Figure 17. Level crossing resonances observed on ^{199}Hg atoms and corresponding to the level crossing occuring near $\omega_0 = 4\omega$ in Fig. 16 (V_1 is the rf voltage, proportional to ω_1).

that the g factor of the dressed atom, g_d, is related to the g factor of the free atom, g, by the expression

$$g_d = gJ_0(\omega_1/\omega) \tag{16}$$

where J_0 is the zeroth-order Bessel function. This effect can be important. For example, for all the values of ω_1/ω corresponding to the zero's of J_0, the dressed atom has no magnetic moment. This modification of g due to the nonresonant coupling with a filled mode of the electromagnetic field may be compared to the well-known g-2 effect (anomalous spin moment of the electron) due to the coupling with the vacuum electromagnetic fluctuations.

If the slope of the levels near $\omega_0 = 0$ is reduced, the width of the zero-field level crossing resonance discussed in the first part of this paper must increase. We have observed such a broadening on ^{199}Hg atoms (Fig. 18).

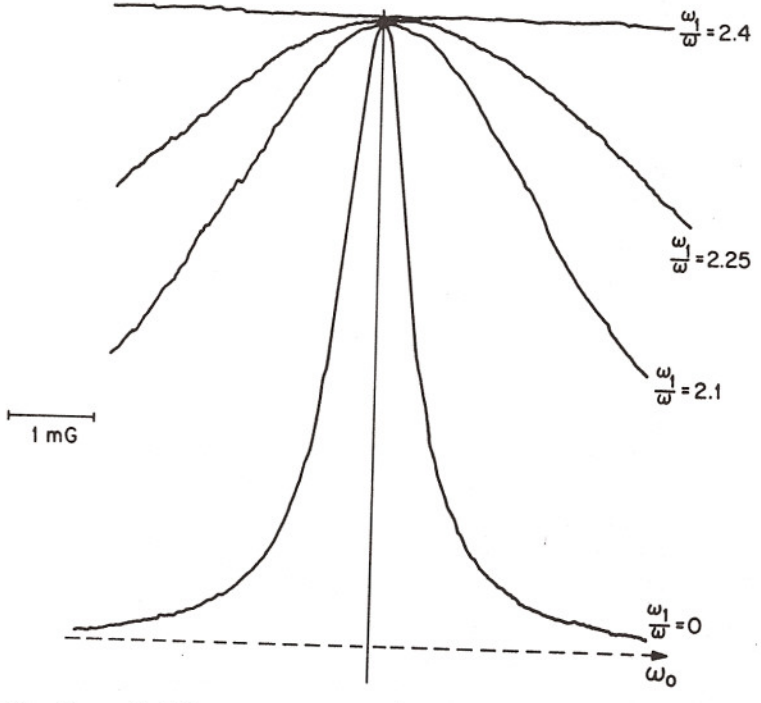

Figure 18. Zero-field level crossing of ^{199}Hg "dressed" atoms. The rf field is linearly polarized. The width of the curves is inversely proportional to g_d; it becomes infinite for the value of ω_1/ω corresponding to the first zero of J_0 [see Eq. (16)].

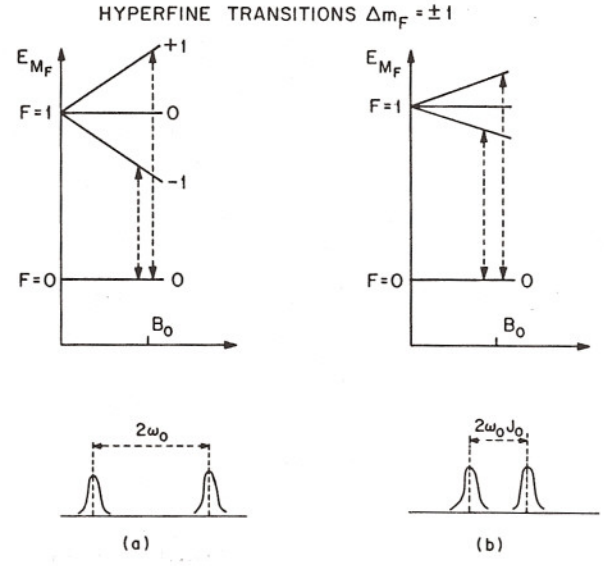

Figure 19. $\Delta m_F = \pm 1$ hyperfine transitions of hydrogen atoms. (a) Free H atoms in a static field B_0; (b) "dressed" H atoms in the same static field B_0. The splitting between the 2 lines is reduced by a factor J_0.

Each curve of Fig. 18 corresponds to a given value of ω_1/ω. One sees that for $\omega_1/\omega = 2.4$ (first zero of J_0), the width of the level crossing resonance becomes infinite. This modification of the g factor has also important consequences on the hyperfine spectrum of hydrogen and alkali atoms. Figure 19 shows the splitting S_0 between the two hyperfine $\Delta m_F = \pm 1$ transitions of H; S_0 is proportional to ω_0 [in weak magnetic fields; See Fig. 19(a)]. If we "dress" the atom by a nonresonant linear rf field, the slope of the F = 1 sublevels decreases and the splitting S between the two $\Delta m_F = \pm 1$ transitions is reduced by a factor $J_0(\omega_1/\omega)$ [see Fig. 19(b)]. The same effect exists also for alkali atoms. We have already mentioned that the two g factors of the F = 2 and F = 1 hyperfine levels are opposite. As J_0 is an even function, the reduction of the slope of the sublevels is the same in both hyperfine levels. It follows that the splitting between the four $\Delta m_F = \pm 1$ hyperfine transitions is reduced as in the hydrogen case. The four lines coalesce for all the zero's of J_0. This appears clearly in Fig. 20 which represents the evolution of the observed hyperfine spectrum of ^{87}Rb atoms interacting with a nonresonant linear rf field of increasing amplitude [21].

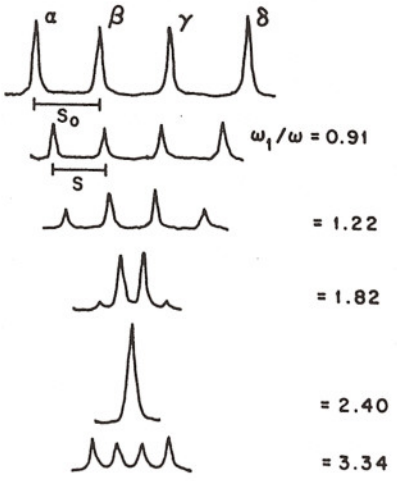

Figure 20. Evolution of the four $\Delta m_F = \pm 1$ hyperfine transitions of ^{87}Rb atoms "dressed" by a nonresonant linear rf field of increasing amplitude. Experimental results. For $\omega_1/\omega = 2.4$ (first zero of J_0), the four lines coalesce.

Figure 21 shows the comparison between the experimentally determined ratios S/S_0 measured on H and ^{87}Rb atoms, and the theoretical variations of the Bessel function J_0.

This possibility of changing continuously the g factor of an atom may provide interesting applications. It has been used, for example, to reduce the effect of static field inhomogeneities on the width of the hyperfine lines. Figure 22(a) shows the hyperfine line $F = 2$, $m_F = 0 \longleftrightarrow F = 1$, $m_F = 0$ of ^{87}Rb broadened by an applied static field gradient. One observes [10] a narrowing of the line [Fig. 22(b)] when the magnetic moment of the ^{87}Rb atoms is reduced when interacting with a nonresonant linear rf field.

Another application [22] is to allow a coherence transfer between two atomic levels with different g factors: by changing the two g factors through the coupling with a nonresonant linear rf field, one can match the Larmor frequencies in the two atoms and make the coherence transfer possible in nonzero magnetic fields.

I hope that these few example will have proven the versatility of optical pumping techniques and the usefulness of concepts such as the one of dressed atoms. It would be interesting to see if they could be generalized to other fields of research.

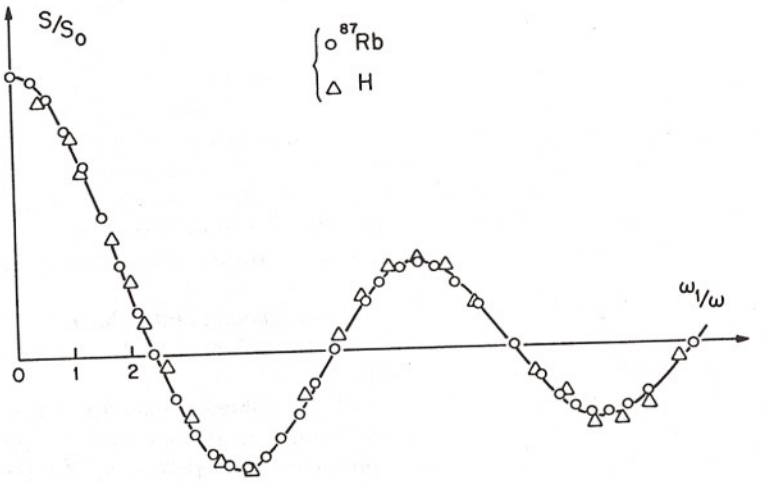

Figure 21. Plot of the ratio S/S_0 versus ω_1/ω. The experimental points for ^{87}Rb and H fit into the same theoretical curve.

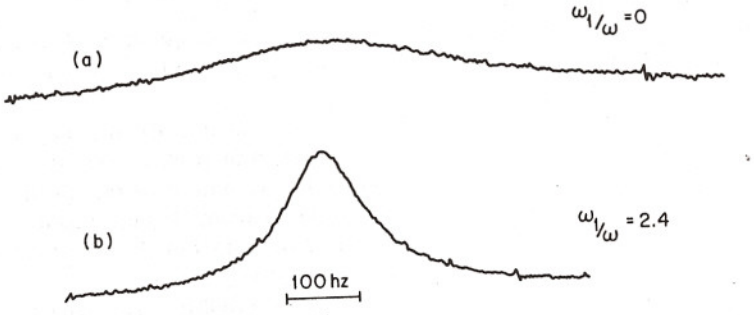

Figure 22. (a) Recording of the $F = 2$, $m_F = 0 \longleftrightarrow F = 1$, $m_F = 0$ hyperfine line of ^{87}Rb atoms broadened by an applied static field gradient. (b) Narrowing of the line when the atoms are "dressed" by a nonresonant linear rf field which cancels the g factor in both hyperfine levels.

REFERENCES

1. For a review article on Optical Pumping, see J. Brossel, in Quantum Optics and Electronics, Les Houches, 1964, (Gordon and Breach, New York, 1965). A. Kastler and C. Cohen-Tannoudji, Progress in Optics, edited by E. Wolf (North-Holland, Amsterdam, 1966), Vol. 5, p. 1.
2. W. Hanle, Z. Phys. 30, 93 (1924); F. D. Colegrove, P. A. Franken, R. R. Lewis, and R. H. Sands, Phys. Rev. Letters 3, 420 (1959).
3. See the review article by Zu Putlitz in Atomic Physics, Proceedings of the First International Conference on Atomic Physics (Plenum Press, New York, 1969), p. 227.
4. Level crossing resonances in atomic ground states have first been observed on ^{111}Cd and ^{113}Cd. J. C. Lehmann and C. Cohen-Tannoudji, Compt. Rend. 258, 4463 (1964).
5. J. Dupont-Roc, S. Haroche, and C. Cohen-Tannoudji, Phys. Letters 28A, 638 (1969); C. Cohen-Tannoudji, J. Dupont-Roc, S. Haroche, and F. Laloe, Revue Phys. Appliquee 5, 95 (1970); 5, 102 (1970).
6. M. A. Bouchiat and J. Brossel, Phys. Rev. 147, 41 (1966).
7. For optical pumping of ^{3}He see F. D. Colegrove, L. D. Schearer, and G. K. Walters, Phys. Rev. 132, 2567 (1963).
8. C. Cohen-Tannoudji, J. Dupont-Roc, S. Haroche, and F. Laloe, Phys. Rev. Letters 22, 758 (1969).
9. J. Dupont-Roc, Revue Phys. Appliquée 5, 853 (1970); J. Phys. (Paris) 32, 135 (1971).
10. For a general and detailed review on the properties of "dressed" atoms, see S. Haroche, thesis (Paris, 1971) [Ann. Phys. (Paris) 6, 189 (1971); 6, 327 (1971).
11. C. Cohen-Tannoudji and S. Haroche, Compt. Rend. 262, 37 (1966); J. Phys. (Paris) 30, 125 (1969); 30, 153 (1969). See also the article in Polarisation, Matiere et Rayonnement, edited by the French Physical Society (Presses Universitaires de France, Paris, 1969). C. Cohen-Tannoudji, Cargese Lectures in Physics, Vol. 2, edited by M. Lévy (Gordon and Breach, New York, 1967).
12. R. J. Glauber, Phys. Rev. 131, 2766 (1963); 131, 2788 (1963).
13. S. H. Autler and C. H. Townes, Phys. Rev. 100, 703 (1955); C. H. Townes and A. L. Schawlow, Microwave Spectroscopy (McGraw-Hill, New York, 1955), p. 279.
14. M. Ledourneuf, These de troisieme cycle (Universite de Paris, 1971).
15. M. Ledourneuf, C. Cohen-Tannoudji, J. Dupont-Roc and S. Haroche, Compt. Rend. 272, 1048 (1971); 272, 1131 (1971). Let us mention that the effect of a nonresonant circularly polarized optical irradiation can also be described in terms of fictitious static fields. See C. Cohen-Tannoudji and J. Dupont-Roc, Phys. Rev. 5, 968 (1972).

16. F. Bloch and A. Siegert, Phys. Rev. 57, 522 (1940).
17. J. M. Winter, thesis (Paris, 1958); Ann. Phys. (Paris), 4, 745 (1959).
18. C. Cohen-Tannoudji and S. Haroche, Compt. Rend. 261, 5400 (1965).
19. N. Polonsky and C. Cohen-Tannoudji, J. Phys. (Paris) 26, 409 (1965).
20. C. Cohen-Tannoudji and S. Haroche, Compt. Rend. 262, 268 (1966). See also Ref. 10
21. S. Haroche, C. Cohen-Tannoudji, C. Audoin, and J. P. Schermann, Phys. Rev. Letters 24, 861 (1970).
22. S. Haroche and C. Cohen-Tannoudji, Phys. Rev. Letters 24, 974 (1970).